arXiv:hep-ph/0511199v2 3 May 2006

Exotic Quark Production in ep Collisions

A. T. Alan, A. Senol and N. Karagoz

Department of Physics, Abant Izzet Baysal University, 14280, Bolu, Turkey

Abstract

We investigate the single production and decay of charge -1/3 ,weak isosinglet vectorlike exotic D quarks in string inspired E_6 theories at future ep colliders; THERA with $\sqrt{s}$=1 TeV, $L = 40$ pb^{-1} and CERN Large Hadron Electron Collider (LHeC) with $\sqrt{s}$=1.4 TeV, $L = 10^4$ pb^{-1}. We found that an analysis of the decay modes of D should probe the mass ranges of 100-450 GeV and 100-1200 GeV at the center of mass energies, 1 and 1.4 TeV , respectively.

PACS numbers: 12.60.-i, 13.60.-r

I. INTRODUCTION

String inspired E_6 theories predict existence of exotic particles. In E_6, each generation of fermions is assigned to the 27-dimensional representation [1, 2]. The presence of additional fermions causes Flavor Changing Neutral Current (FCNC) interactions and possible deviations from weak universality in Charged Current (CC) [3]. In this study we consider exotic down quark (D), a charge -1/3, quark which is a weak isosinglet particle.

Production of exotic quarks have been studied at HERA [4, 5] and LEP [6] energies as CC and FCNC reactions. We analyze the possible production of these quarks and some of their indirect signatures including the contributions of boson-gluon fusions [7] at two future high energy ep collider options; THERA with $\sqrt{s}$=1 TeV and $L = 40\ pb^{-1}$ [8] and CERN Large Hadron Electron Collider (LHeC) with $\sqrt{s}$=1.4 TeV and $L = 10^4\ pb^{-1}$ at which 7 TeV LHC protons collide with 70 GeV ring electron or positron beam [9]. These colliders complement the hadron collider programmes and provide new discovery potential to them. A relatively high integrated luminosity of 10 fb^{-1} at the LHeC makes an essential facility to resolve possible puzzles of the LHC data.

II. PRODUCTION AND DECAYS OF D

The single production of exotic down quarks occur via the following t-channel subprocesses in ep collisions as shown in Fig. 1;
i) Charged Current reaction; $eu \to \nu_e D$
ii) FCNC reaction; $ed \to eD$
iii) Boson-Gluon Fusions; $Wg \to \bar{u}D$, $Zg \to \bar{d}D$ and $\gamma g \to \bar{d}D$.
The CC and FCNC interactions for the exotic D quarks mixed with standard fermions and standard bosons W, Z are given by

$$\mathcal{L}_{CC} = \frac{g}{2\sqrt{2}}\bar{u}\gamma_\mu(1-\gamma_5)(d\cos\theta - D\sin\theta)W^\mu + h.c. \tag{1}$$

$$\mathcal{L}_{NC} = \frac{g}{4c_W}\sin\theta\cos\theta\bar{d}\gamma_\mu(1-\gamma_5)DZ^\mu \tag{2}$$

where θ are the mixing angels between the ordinary quarks and the exotic down quarks, g denotes the gauge coupling relative to SU(2) symmetries.

As we consider the strong interactions, D quarks couple to gluons in exactly the same

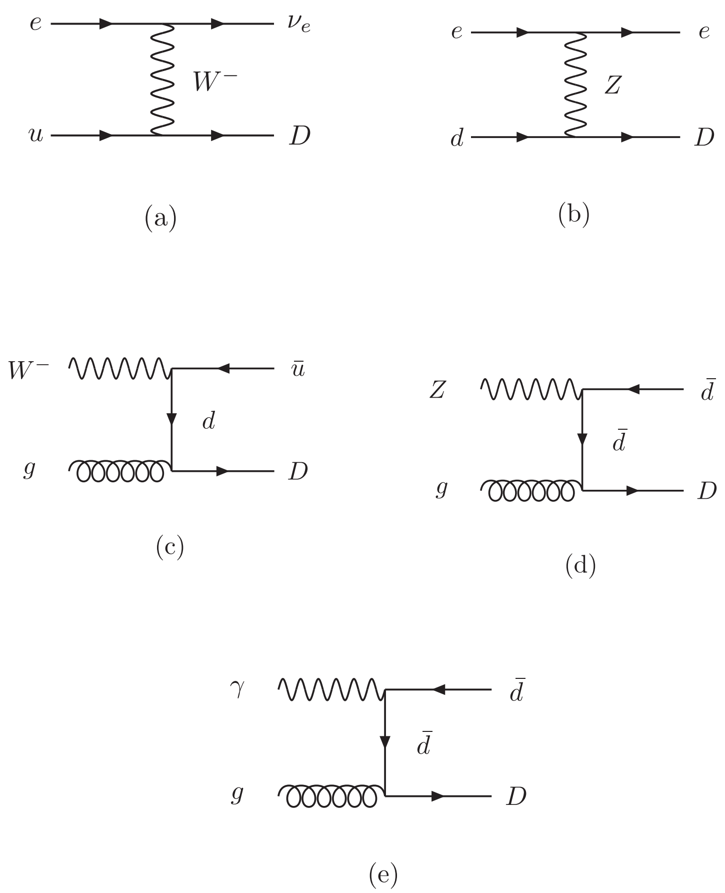

(a) (b) (c) (d) (e)

FIG. 1: The Feynman diagram at parton level for single exotic down quark production in ep collisions via (a) charged current interaction (b) neutral current interaction (c) W-gluon fusion (d) Z-gluon fusion (e) γ-gluon fusion

way as ordinary quarks providing the (W, Z, γ)-gluon fusions. Corresponding differential cross sections are written as follows:

$$\begin{aligned}
\frac{d\hat{\sigma}}{d\hat{t}}(eu \to \nu_e D) &= \frac{\pi\alpha^2 \sin^2\theta}{4\sin^4\theta_W \hat{s}[(\hat{t}-M_W^2)^2+\Gamma_W^2 M_W^2]}[(\hat{s}-m^2)] \\
\frac{d\hat{\sigma}}{d\hat{t}}(ed \to eD) &= \frac{\pi\alpha^2 \sin^2 2\theta[\hat{t}(\hat{t}+2\hat{s}-m^2)(a_e-v_e)^2+2\hat{s}(\hat{s}-m^2)(a_e^2+v_e^2)]}{4\hat{s}^2\sin^4 2\theta_W[(\hat{t}-M_Z^2)^2+\Gamma_Z^2 M_Z^2]} \\
\frac{d\hat{\sigma}}{d\hat{t}}(Wg \to \bar{u}D) &= \frac{\pi\alpha_s\alpha\cos^2\theta}{32\hat{s}^2\hat{t}^2 M_W^2}[2M_W^4(m^2+\hat{t})-2M_W^2\hat{t}(\hat{s}+\hat{t})-(m^2-\hat{s})\hat{t}^2] \\
\frac{d\hat{\sigma}}{d\hat{t}}(Zg \to \bar{d}D) &= \frac{\pi\alpha_s\alpha(a_d^2+v_d^2)}{8\sin^2 2\theta_W\hat{s}^2\hat{t}^2 M_Z^2}[2M_Z^4(m^2+\hat{t})-2M_Z^2\hat{t}(\hat{s}+\hat{t})-(m^2-\hat{s})\hat{t}^2] \\
\frac{d\hat{\sigma}}{d\hat{t}}(\gamma g \to \bar{d}D) &= \frac{\pi\alpha_s\alpha}{24\hat{s}^2\hat{t}}[-\hat{s}-\hat{t}]
\end{aligned} \tag{3}$$

here M_W, M_Z and Γ_W, Γ_Z are masses and decay widths of a W and Z bosons. $a_e(a_d)$ and $v_e(v_d)$ stand for axial and vector coupling constants of electron (down quark) and m refers to D masses.

The total production cross section is obtained by folding the partonic cross section over the parton distributions in the proton. In numerical calculations of the total cross sections we have used the MRST parametrization [10] for the partons and the Weizsäcker-Williams distribution [11, 12] for photons in electrons. For illustrations we have assumed an upper bound of $\sin^2\theta \lesssim 0.05$ in numerical calculations which is appropriate as being at the order of CKM angle. The calculated total cross sections corresponding to five subprocess have been displayed in Figures 2-6 as functions of D masses m for two center of mass energies. In these figures solid (dashed) lines are for $\sqrt{s}$=1.4 (1) TeV. In Tables I and II, we present the total production cross sections of the five reactions for various masses at THERA and LHeC, respectively. As can be seen, for 100-300 GeV D quarks Z-gluon and γ-gluon fusions are dominant reactions but for higher mass range contributions of these fusions decrease very fast.

Since these exotic quarks must be at a scale well above 100 GeV [13], the main decays of them would be $D \to dZ$ and $D \to uW$ and partial decay widths can be written as

$$\Gamma(D \to qV) = \alpha C_V \frac{m}{Y^2}(1 - 3Y^4 + 2Y^6) \tag{4}$$

where q is up or down quark, V denotes W^- and Z bosons, α is the fine structure constant, $Y \equiv M_V/m$, $C_W = \sin^2\theta/8x_W$, $C_Z = (\sin\theta\cos\theta)^2/16x_W(1-x_W)$ and $x_W \equiv \sin^2\theta_W$. Eq. (4) gives rise to branching ratios of BR($D \to dZ$)=30 % and BR($D \to uW$)= 70 % which do not change significantly depending on D masses, as seen from Table III. Therefore, $D \to ul^-\bar{\nu}_l$ is taken as the relevant background process since the $D \to uW$ is dominant one. In Tables IV and V we present the cross sections resulting the background processes (considering only the first generation of leptons) for $\sqrt{s}$=1 and 1.4 TeV, respectively. Results reported in these tables were obtained by using the high energy package CompHEP [14] along with CTEQ6L [15] which has been used in the background calculations and an optimal cut of $P_T > 10$ GeV has taken for electron, jet and missing momenta.

In Figure 7, we displayed the transverse momenta, P_T of secondary electrons by assigning a mass value of 350 GeV to m giving peaks around P_T^e=30-40 GeV and the invariant mass distributions of $e\!-\!\bar{\nu}_e\!-\!q$ system resulting from the decay of D quarks for the five subreactions separately. These invariant mass spectra have Jacobian peaks of around 125-200 GeV. Similarly, in Figure 8 the transverse momenta and invariant mass distributions are displayed for LHeC energy which yields peaks around 20-40 GeV for P_T^e values and 125-350 GeV for invariant mass values depending on different subprocess.

III. CONCLUSION

We have investigated charge -1/3 weak isosinglet vectorlike quarks predicted by E_6 theories. We found that a very clear signature for the semileptonic $e\nu_e u$ final state at two high energy electron-proton colliders options THERA and LHeC is possible. As presented in Tables IV and V the background cross sections varies in the range of the order of $10^{-3} - 10^{-7}$ *pb* at THERA for 500 GeV quarks and $10^{-5} - 10^{-9}$ *pb* at LHeC for 1000 GeV quarks. As seen from Tables VI and VII, exotic quark masses can be as high as 450 GeV and 1.2 TeV at the center of mass energies of $\sqrt{s} = 1$ and 1.4 TeV, respectively, taking $S/\sqrt{S+B} > 5$, S is the number of signals and B is that of background events, as an observation limit of signal. In obtaining these numerical values, we have taken an appropriate mixing angle value of $\sin^2\theta$=0.05 which is at the order of the angle in the CKM matrix.

Acknowledgments

This work is partially supported by Abant Izzet Baysal University Research Fund.

---

[1] T. G. Rizzo, Phys. Rev. D **34**, 1438 (1986).

[2] J. L. Hewett and T. G. Rizzo, Phys. Rept. **183**, 193 (1989).

[3] V. D. Barger, N. Deshpande, R. J. N. Phillips and K. Whisnant, Phys. Rev. D **33**, 1912 (1986) [Erratum-ibid. D **35**, 1741 (1987)].

[4] J. L. Hewett, Phys. Lett. B **196**, 223 (1987).

[5] F. M. L. Almeida, J. A. Martins Simoes, C. M. Porto, P. P. Queiroz and A. J. Ramalho, Phys. Rev. D **50** (1994) 5627.

[6] T. G. Rizzo, Phys. Rev. D **40**, 754 (1989).

[7] G. A. Schuler, Nucl. Phys. B **299**, 21 (1988).

[8] H. Abramowicz *et al.* [TESLA-N Study Group] DESY-01-011.

[9] J. B. Dainton, M. Klein, P. Newman, E. Perez and F. Willeke, arXiv:hep-ex/0603016.

[10] A. D. Martin, R. G. Roberts, W. J. Stirling and R. S. Thorne, Eur. Phys. J. C **4**, 463 (1998).

[11] C. F. von Weizsacker, Z. Phys. **88**, 612 (1934).

[12] E. J. Williams, Phys. Rev. **45**, 729 (1934).

[13] S. Eidelman *et al.* [Particle Data Group], Phys. Lett. B **592**, 1 (2004).

[14] A. Pukhov *et al.*, arXiv:hep-ph/9908288.

[15] H. L. Lai *et al.*, Phys. Rev. D **51**, 4763 (1995).

TABLE I: The total cross sections in *pb* for the signal processes for the exotic quarks at THERA.

m(GeV)	100	200	300	400	500
$\sigma_S(eu \to \nu_e D)$	4.01	2.84	1.79	0.99	0.46
$\sigma_S(ed \to eD)$	0.27	0.18	0.11	0.053	0.022
$\sigma_S(Wg \to \bar{u}D)$	3.16	1.25	0.39	0.10	0.019
$\sigma_S(Zg \to \bar{d}D)$	23.95	9.30	2.91	0.73	0.14
$\sigma_S(\gamma g \to \bar{d}D)$	59.62	9.78	1.73	0.29	0.041

TABLE II: The total cross sections in *pb* for the signal processes for the exotic quarks at LHeC.

m(GeV)	200	400	600	800	1000
$\sigma_S(eu \to \nu_e D)$	3.61	1.97	0.83	0.24	0.036
$\sigma_S(ed \to eD)$	0.25	0.12	0.044	0.011	0.0013
$\sigma_S(Wg \to \bar{u}D)$	2.09	0.45	0.061	0.0048	1.79x10^{-4}
$\sigma_S(Zg \to \bar{d}D)$	16.14	3.49	0.47	0.037	1.42x10^{-3}
$\sigma_S(\gamma g \to \bar{d}D)$	15.16	1.23	0.094	0.0049	1.42x10^{-4}

TABLE III: The branching ratios for D decays.

m(GeV)	BR($D \to qW$)	BR($D \to qZ$)
150	70.2 %	29.2%
250	68.1%	31.9%
350	67.8%	32.1%
450	67.7%	32.3%

TABLE IV: The total cross sections for the background processes for the exotic quarks at THERA.

m(GeV)	100	200	300	400	500
$\sigma_B(eu \to \nu_e\, e\, \bar{\nu}_e\, u)$	1.122x10^{-3}	1.451x10^{-3}	4.238x10^{-4}	1.856x10^{-4}	8.976x10^{-5}
$\sigma_B(ed \to e\, e\, \bar{\nu}_e\, u)$	8.349x10^{-4}	1.095x10^{-3}	3.332x10^{-4}	8.996x10^{-4}	1.195x10^{-3}
$\sigma_B(Wg \to \bar{u}\, e\, \bar{\nu}_e\, u)$	2.011x10^{-3}	2.556x10^{-2}	7.473x10^{-2}	2.578x10^{-2}	1.425x10^{-4}
$\sigma_B(Zg \to \bar{d}\, e\, \bar{\nu}_e\, u)$	1.502x10^{-3}	7.417x10^{-3}	8.200x10^{-3}	3.843x10^{-5}	5.511x10^{-4}
$\sigma_B(\gamma g \to \bar{d}\, e\, \bar{\nu}_e\, u)$	5.071x10^{-3}	1.195x10^{-3}	3.196x10^{-4}	2.860x10^{-5}	7.210x10^{-7}

TABLE V: The total cross sections in pb for background processes for the exotic quarks at LHeC.

m(GeV)	200	400	600	800	1000
$\sigma_B(eu \to \nu_e\, e\, \bar{\nu}_e\, u)$	1.852x10^{-3}	5.002x10^{-4}	2.157x10^{-4}	3.405x10^{-5}	7.724x10^{-6}
$\sigma_B(ed \to e\, e\, \bar{\nu}_e\, u)$	8.398x10^{-4}	5.814x10^{-5}	4.309x10^{-5}	4.619x10^{-6}	1.128x10^{-6}
$\sigma_B(Wg \to \bar{u}\, e\, \bar{\nu}_e\, u)$	5.976x10^{-3}	5.260x10^{-3}	3.330x10^{-4}	2.352x10^{-4}	2.786x10^{-5}
$\sigma_B(Zg \to \bar{d}\, e\, \bar{\nu}_e\, u)$	7.938x10^{-3}	1.399x10^{-2}	1.048x10^{-3}	9.683x10^{-6}	3.436x10^{-5}
$\sigma_B(\gamma g \to \bar{d}\, e\, \bar{\nu}_e\, u)$	1.369x10^{-3}	1.090x10^{-5}	1.239x10^{-5}	2.512x10^{-8}	1.114x10^{-9}

TABLE VI: The significance ($S/\sqrt{S+B}$) for the exotic quarks at THERA ($L = 40\ pb^{-1}$).

m(GeV)	100	200	300	400	500
$eu \to \nu_e D$	12.66	10.65	8.46	6.29	4.30
$ed \to eD$	3.28	2.68	2.05	1.46	0.94
$Wg \to \bar{u}D$	11.24	7.00	3.64	1.77	0.87
$Zg \to \bar{d}D$	30.94	19.28	10.78	5.40	2.39
$\gamma g \to \bar{d}D$	48.83	19.78	8.31	3.40	1.28

TABLE VII: The significance ($S/\sqrt{S+B}$) for the exotic quarks at LHeC ($L = 10^4\ pb^{-1}$).

m(GeV)	200	400	600	800	1000
$eu \to \nu_e D$	189.95	140.33	91.04	48.91	18.87
$ed \to eD$	49.58	34.85	21.67	10.35	3.54
$Wg \to \bar{u}D$	144.62	66.93	24.61	6.75	1.25
$Zg \to \bar{d}D$	401.64	186.42	68.62	19.32	3.72
$\gamma g \to \bar{d}D$	389.33	111.03	30.65	7.00	1.19

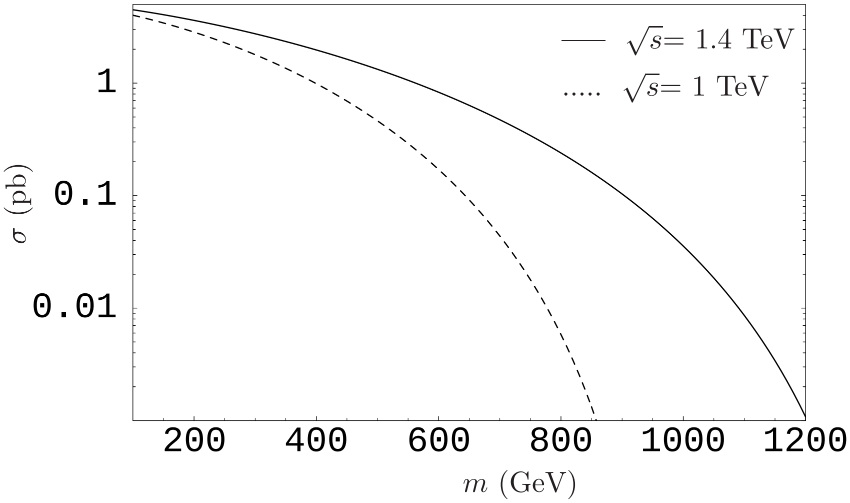

FIG. 2: The total production cross sections for the subprocesses $eu \to \nu_e D$ as a functions of m.

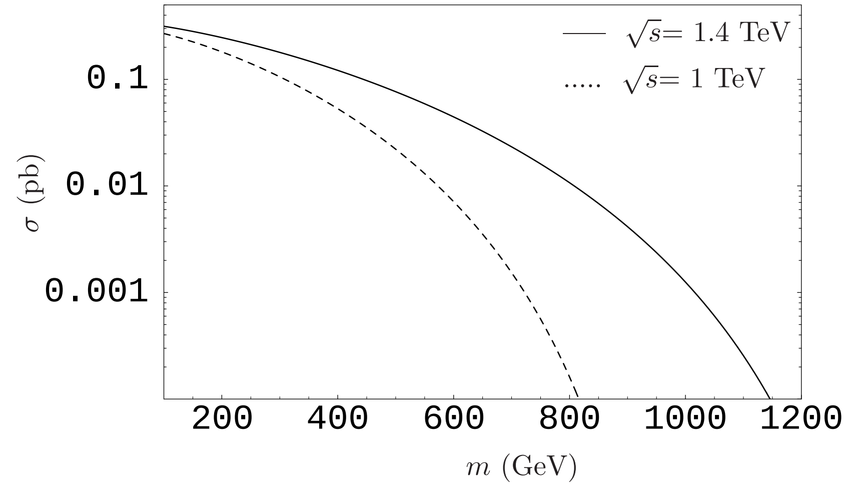

FIG. 3: The total production cross sections for the subprocesses $ed \to eD$ as a functions of m.

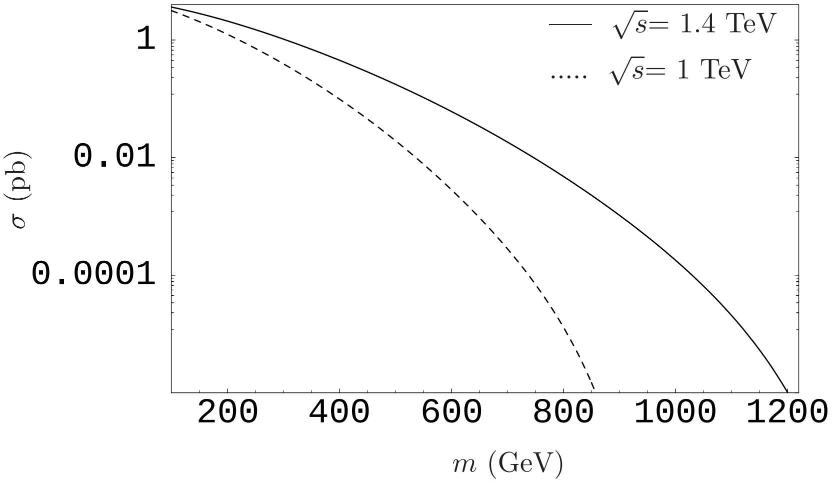

FIG. 4: The total production cross sections for the subprocesses $Wg \to \bar{u}D$ as a functions of m.

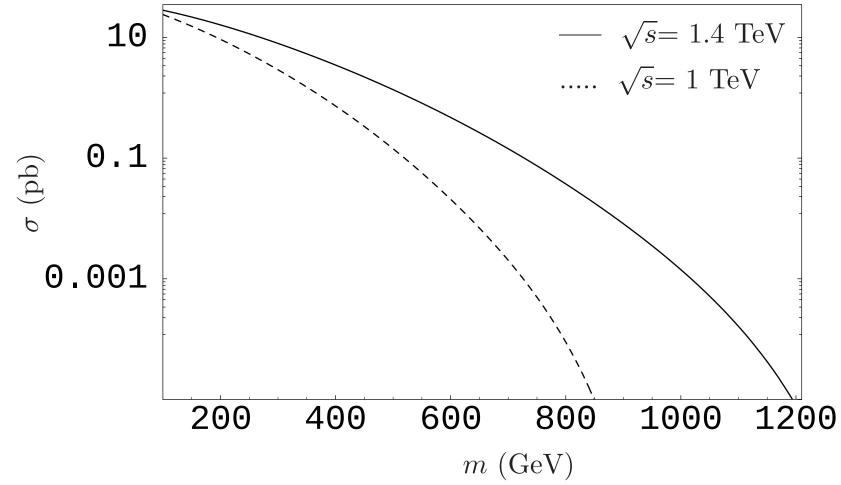

FIG. 5: The total production cross sections for the subprocesses $Zg \to \bar{d}D$ as a function of m.

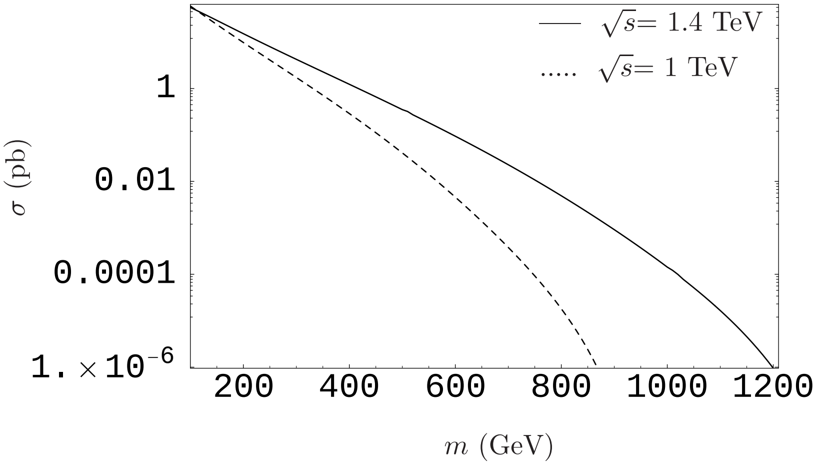

FIG. 6: The total production cross sections for the subprocesses $\gamma g \to \bar{d}D$ as a functions of m.

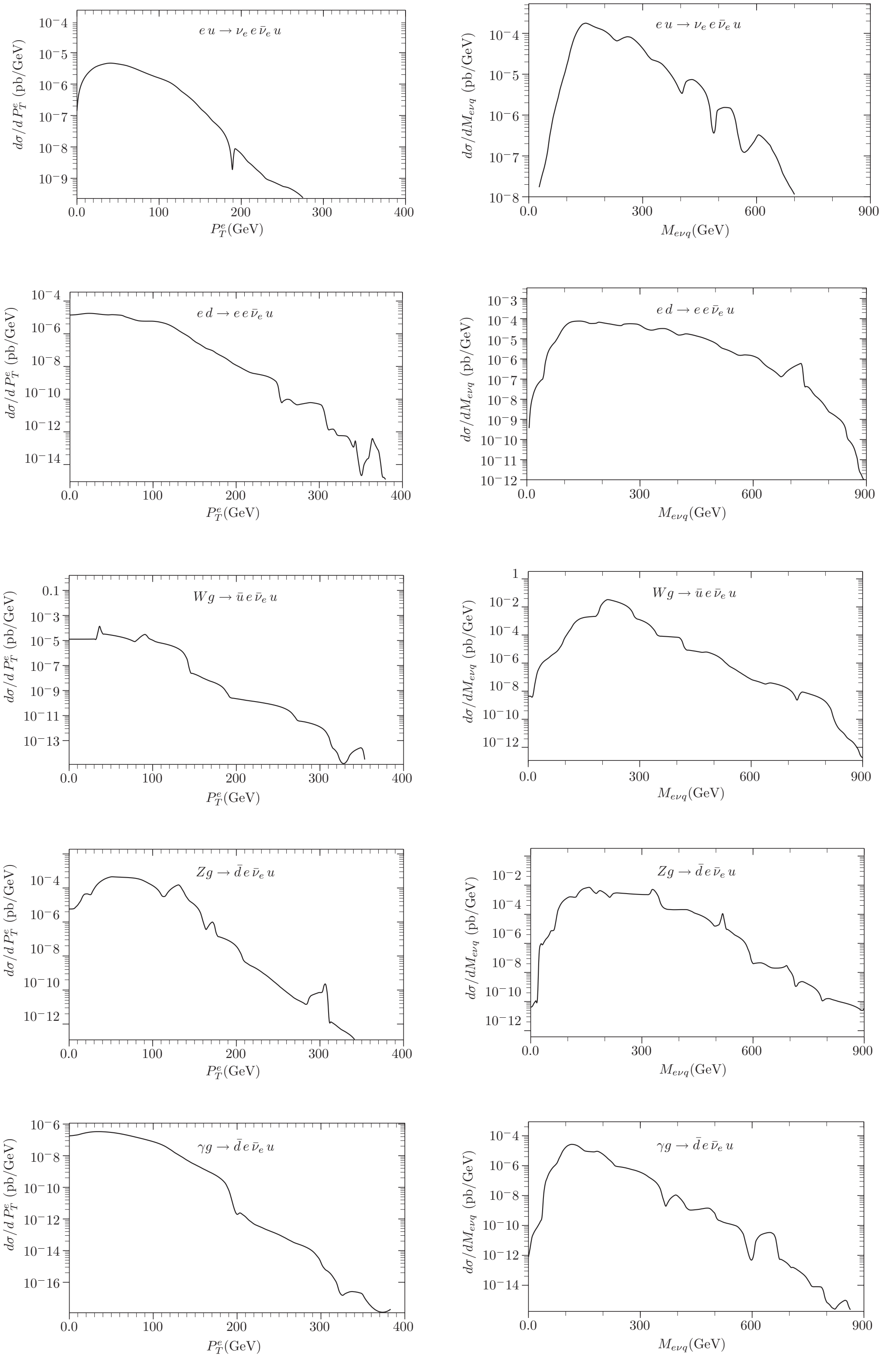

FIG. 7: Transverse momentum P_T^e and invariant mass distributions of the backgrounds at THERA($\sqrt{S}$=1 TeV).

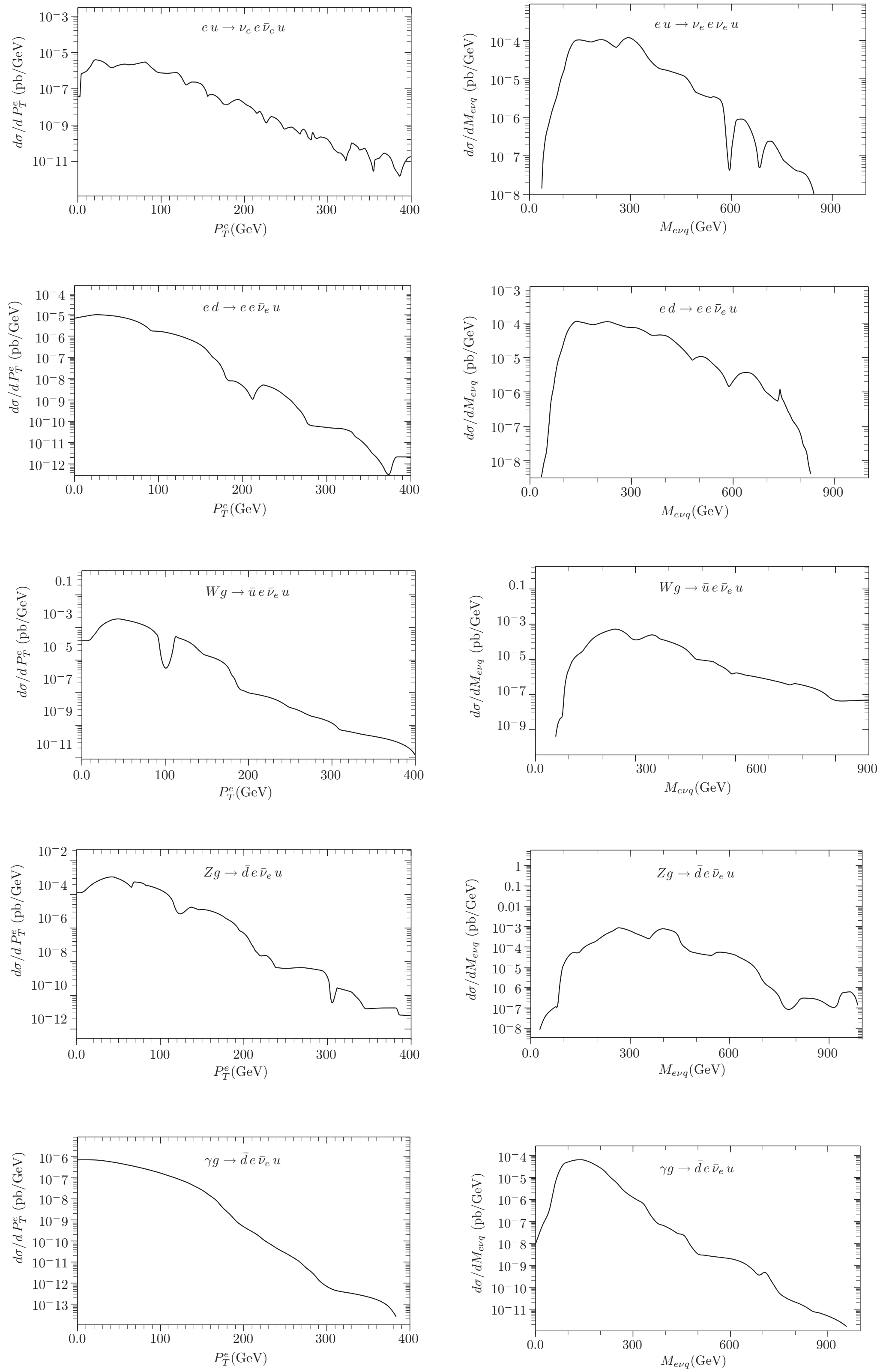

FIG. 8: Transverse momentum P_T^e and invariant mass distributions of the backgrounds at LHeC($\sqrt{S}$=1.4 TeV).